Measuring lateral and vertical electromagnetic velocity in the vadose zone using GPR reflection tomography

John H. Bradford, CGISS, Boise State University

Introduction

Accurate estimation of electromagnetic (EM) velocity is critical in ground penetrating radar investigations. Not only does the velocity enable accurate time to depth image transforms, but the velocity is a direct measure of subsurface electrical properties that may be used to improve our understanding of the subsurface. When coupled with a suitable mixing equation, the velocity can be used to estimate dielectric permittivity which in turn may lead to estimates of pore fluid content (Greaves et al., 1996; Huisman et al., 2003; Topp et al., 1980). By acquiring continuous CMP profiles, it is possible to measure laterally and vertically continuous GPR velocity profiles (Greaves et al., 1996). With this method the well established acquisition geometries of seismic exploration are used to acquire several traces, with varying source-receiver separations, at each point within a survey. Additionally these data have a number of advantages over conventional fixed offset GPR data including improved suppression of coherent and random noise (Liberty and Pelton, 1994; Pipan et al., 1999; Pipan et al., 2003).

NMO based processing schemes are subject to the fundamental assumptions of NMO velocity analysis which include small offset-to-depth ratios, small vertical and horizontal velocity gradients, and planar flat lying reflections. These assumptions are often violated in GPR investigations. For example, EM velocity can decrease by a factor of 2 or more across the water table as the sediment grades from dry to full water saturation (Bradford, 2003; Bradford, 2004). This can result in severe departure from normal moveout leading to large overestimates of interval velocity (Bradford, 2002). When NMO velocity analysis fails, more rigorous methods of velocity estimation are required.

Migration velocity analysis

Prestack depth migration (PSDM) depends strongly on the depth velocity model so that accurate velocity estimation is critical. Methods for estimating the velocity distribution fall into two categories: 1) Reflection tomography, and 2) PSDM velocity analysis.

Most tomography algorithms are designed to invert for the velocity structure based on travel time picks of specific reflecting horizons in the premigration domain. As pointed out by Stork (1992), tomography has the advantage that computational methods for solving the inverse problem are well understood and solutions can be found quickly and efficiently. A significant disadvantage arises when there is significant subsurface complexity and wavefield distortion makes it difficult to pick the traveltimes of specific reflecting horizons.

PSDM velocity analysis takes advantage of the strong velocity dependence of PSDM. When the data are migrated with the correct velocity model, reflections in common image point (CIP) gathers (the post-migration analog of CMP gathers) will migrate to the same depth and will appear flat. If the velocity model is wrong, there is an apparent offset dependent depth which can be characterized as residual moveout (RMO). The RMO is positive or negative depending on whether the velocity is too high or too low respectively. After migration with an initial velocity model, the velocity model is updated to remove RMO with a top-to-bottom method known as layer stripping. With this method the data are remigrated after each velocity update and checked for RMO, often using coherence panels in the CIP domain (Lafond and Levander, 1993). The process is repeated until all RMO is removed. PSDM analysis takes advantage of reflector coherence and continuity in the postmigration domain. This improves the processor's ability to evaluate specific reflecting horizons, particularly in a complex subsurface setting. Further, the output of PSDM velocity analysis is a suburface velocity model and PSDM image.

Both reflection tomography and PSDM velocity analysis have been applied to ground-penetrating radar data. For example, Cai and McMechan (1999) describe a method for estimating the subsurface EM velocity and attenuation models using a reflection tomography algorithm. Leparoux et al. (2001) discuss the application of PSDM migration velocity analysis to GPR data.

Stork (1992) presents a method of reflection tomography that seeks to minimize RMO in CIP gathers in the post-migration domain. This method combines the computational advantages of tomography with the inherent interpretational advantage of PSDM velocity analysis. Reflection tomography in the postmigration domain is a robust tool and the software needed to implement this method is commercially available and convenient to use. While more commonly applied in seismic reflection data processing, such tools are rarely used in GPR data analysis. As with most forms of geophysical inversion, it is not a "black box"

process and requires careful quality control by the data processor.

Here I summarize the results of two field experiments taken from contaminated site investigations at the Department of Energy's (DOE) Hanford site, Washington, and a former refinery near Cincinnati, Ohio. In both case studies, I use Stork's (1992) method to construct detailed velocity models from multi-fold GPR data sets.

Cincinnati, Ohio Refinery Site

At this site, an estimated minimum of 4,000,000 gallons of leaded gasoline and diesel fuel were released to the environment from the early 1930s to the early 1980s. This contaminant now forms a thick zone of hydrocarbon contamination that interacts dynamically with the fluctuating water table. Approximately 2,500,000 gallons of contaminant have been removed through extraction wells over the last 10 - 15 years, but a significant source term remains. The water table fluctuates by 3 - 5 m annually. At low water table conditions, the hydrocarbon forms a pool at the top of the water saturated zone, and at high water table conditions, the contaminant remains trapped in the pore space below the water table forming a thick smear zone. The sediment column is variable ranging from course sands and gravels to silty and clay sands. At a depth of 24 m to 30 m a clay aquitard is present. The water table is roughly 9 m - 18 m below the ground surface depending on topographic relief and temporal ground water variations.

In January, 2002 a three person crew acquired approximately

1710 linear m of 2D multi-fold GPR data (50 MHz) consisting of both TE and TM configurations along three transects ranging in length from 152 m to 274 m. Data were acquired at high water table conditions with the contaminant forming a 3 - 5 m thick smear zone and essentially no floating product. Plans were made to revisit the site during low water table conditions, but had to be canceled due to ongoing site development activities.

Data were acquired in 25-fold common-source point mode with 0.6 m source and receiver intervals, 2 m near offset and maximum offset of 17 m. Data quality varied from excellent to poor with penetration of 12 - 25 m. Processing consisted of a time-zero correction, bandpass filtering (12-25-100-200MHz), AGC (30 ns time gate), and 2D PSDM reflection tomography along all profiles. All pre-stack migrations were done in the common-offset domain using a Kirchhoff algorigthm.

Reflection tomography revealed a highly heterogeneous velocity structure in the vadose zone with a large lateral gradient where the fill transitions from gravel to clay sand and the velocity decreases sharply by approximately 30 % (Figure 1). A sharp increase in signal attenuation is also observed at the transition from gravel to clay sand. South of this lithologic change the water table reflection is still evident, but energy does not reach the base of the contaminated interval. Further, I identified reflections from the top and bottom of an interval consistent with the contaminated zone identified in boreholes (Figure 1). From 30 - 120 m, where the overburden is dominated by gravel, elevated velocities are present below the water table within
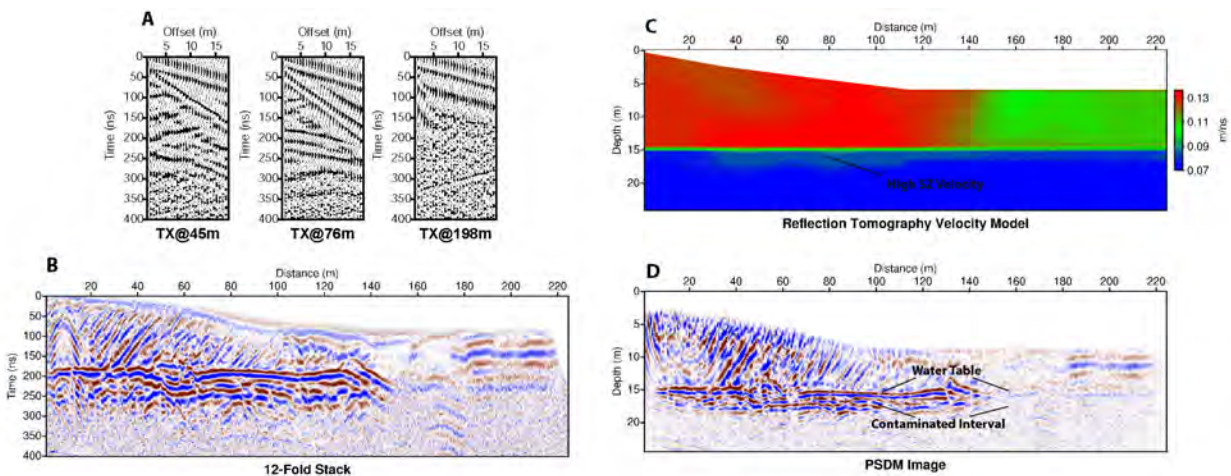

Figure 1: A) Common-source gathers from the Ohio site. Steeply dipping reflections are evident from backdipping moveout (e.g. TX=45 m and 76 m). A significant decrease in surface velocity past 150 m is evident where the dips of the direct ground arrival steepens (e.g. TX=198 m). B) The NMO stack reveals dipping strata in the near surface and a clear reflection from the water table. At distances greater than 150 m the signal is severely degraded due to increased attenuation. Note the approximately 40 ns push down of the water table reflection at distances greater than 150 m. C) Reflection tomography shows an abrupt lateral decrease in near surface velocity starting at a distance of 140 m. D) The water table reflection below the low velocity zone is properly located in depth after PSDM.
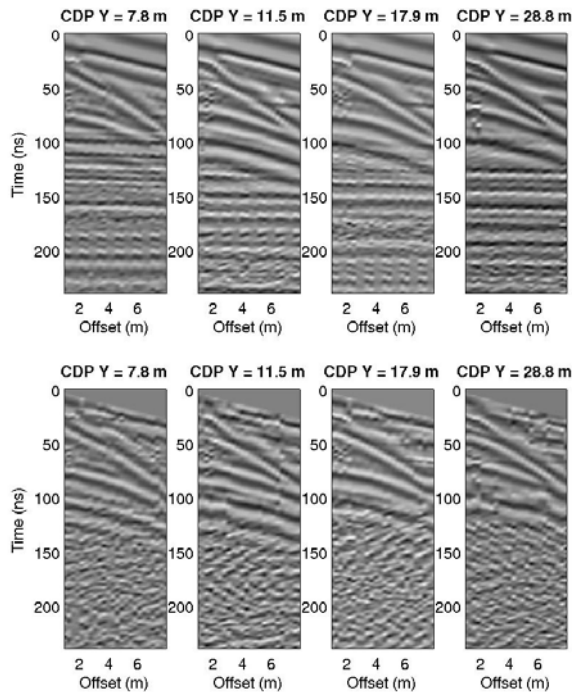
Figure 2: Comparison of CMP gathers from the 3D Hanford site survey before (top) and after (bottom) eigenvector filtering to suppress the air velocity scattering noise. The off-end events are horizontal in the CMP domain and are effectively separated from the subsurface reflections.

the contaminated zone. The velocity decreases further to north where well data indicate a significant decrease in LNAPL concentrations. Determining whether the velocity increase is caused by the LNAPL is complicated by stratigraphic changes that are coincident with the lateral increase in velocity below the water table. The velocity increase is within the range of saturated sediments so we cannot rule out the interpretation of velocity increase as purely due to a lithologic change. However, the high concentrations of LNAPL at this site makes it likely that the presence of contaminant has a strong influence on the velocity distribution. It should be noted that the contaminated interval is ~ one wavelength thick and so, is near the limit of PSDM velocity analysis resolution.

DOE Hanford site, 200W Area

At the DOE Hanford site, carbon tetrachloride (CCl_4) was used extensively in the processing of plutonium. The Z-9 trench in the 200W Area received the majority of CCl_4 at the Hanford site, and is thought to be the primary source area for the CCl_4 plume that now exists below 200W. In April, 2002, the field crew acquired a 3D survey adjacent to the Z-9 trench. The objective of the survey was to identify lateral variability in vadose water content in the upper 10 - 15 m. Shallow sediments at the site consist of sandy fill material (0-

4m) overlying the sands and gravels of the Hanford formation.

The survey patch was 14 m x 27 m. Data were acquired with 100 MHz antennas in 25-fold common-source point gathers with 0.6 m source interval, 0.3 m receiver interval, near offset of 1m and far offset of 8.5 m. Profiles were oriented at 0°, 45°, and 90° relative to the long direction of the 3D patch. The data were combined into 0.45 m CMP bins.

Data processing consisted of a time-zero correction, bandpass filtering (25-50-400-800MHz), AGC (20 ns time gate), eigenvector filtering to attenuate coherent noise from surface scatter, 2D PSDM reflection tomography along all profiles followed by 3D smoothing of the velocity volume, and 3D Kirchhoff prestack time migration. The data were heavily contaminated with coherent noise scattered from surface objects associated with the nearby soil vapor extraction plant. Through eigenvector filtering, the air velocity scatter effectively removed with minimal filtering artifacts (Figure 2).

Velocities generally increase with in-line position and decrease with cross-line position (Figure 3). A low velocity/high water content layer is present between 4 m and 7 m. Detailed NMO analysis with Dix inversion, and reflection tomography produce similar results in the upper 7 m. This similarity is not too surprising, given the relatively smooth velocity gradients and flat lying stratigraphy. However, PSDM velocity analysis is more accurate and the tomographic model a better representation of subsurface properties.

Two, subhorizontal reflections at ~4 m and 6 m dominate radar stratigraphy at the site (Figure 3). Above 4 m, gently dipping horizons are present with some foreset beds. This shallow stratigraphy is related to backfill at the site. The 6 m reflection deepens at low in-line positions. This deepening correlates with an increase in water content (Figure 3). While stratigraphy at the site is relatively simple, tomographic inversion indicates significant lateral and vertical heterogeneity in the near surface water distribution.

References

Bradford, J.H. 2002, Depth characterization of shallow aquifers with seismic reflection - Part I: The failure

of NMO velocity analysis and quantitative error prediction: Geophysics, **67**, 89-97.

Bradford, J.H., 2003, GPR offset-dependent reflectivity analysis for characterization of a high-conductivity LNAPL plume: SAGEEP 2003 Symposium on the Application of Geophysics to Environmental and Engineering Problems, Env. Eng. Geophys. Soc., 238-252.

Bradford, J.H., 2004, 3D Multi-offset, multi-polarization acquisition and processing of gpr data: a controlled DNAPL spill experiment: SAGEEP 2004 Symposium on the Application of Geophysics to Environmental and Engineering Problems, Env. Eng. Geophys. Soc., 514-527.

Cai, J., and McMechan, G.A., 1999, 2-D ray-based tomography for velocity, layer shape, and attenuation from GPR data: Geophysics, **64**, 1579-1593.

Greaves, R.J., Lesmes, D.P., Lee, J.M., and Toksoz, M.N., 1996, Velocity variation and water content estimated from multi-offset, ground-penetrating radar: Geophysics, **61**, 683-695.

Huisman, J.A., Hubbard, S.S., Redman, J.D., and Annan, A.P., 2003, Measuring soil water content with ground-penetrating radar: A review: Vadose Zone Journal, **2**, 476-491.

Lafond, C.F., and Levander, A.R., 1993, Migration moveout analysis and depth focusing: Geophysics, **58**, 91-100.

Leparoux, D., Gibert, D., and Cote, P., 2001, Adaptation of prestack migration to multi-offset ground-penetrating radar (GPR) data: Geophys. Prosp., **49**, 374-386.

Liberty, L.M., and Pelton, J.R., 1994, A comparison of ground-penetrating radar methods: multi-fold data vs. single fold data: 30th Symposium on Engineering Geology and Geotechnical Engineering: Hydrogeology, Waste Disposal, Science and Politics, 321-324.

Pipan, M., Baradello, L., Forte, E., Prizzon, A., and Finetti, I., 1999, 2-D and 3-D processing and interpretation of multi-fold ground penetrating data: a case history from an archaeological site: J. Appl. Geophys., **41**, 271-292.

Pipan, M., Forte, E., Dal Moro, M., Sugan, M., and Finetti, I., 2003, Multifold ground-penetrating radar and resistivity to study the stratigraphy of shallow unconsolidated sediments: The Leading Edge, 876-881.

Stork, C., 1992, Reflection tomography in the postmigrated domain: Geophysics, **57**, 680-692.

Topp, G.C., Davis, J.L., and Annan, A.P., 1980, Electromagnetic determination of soil water content; measurements in coaxial transmission lines: Water Resour. Res., **16**, 574-582.
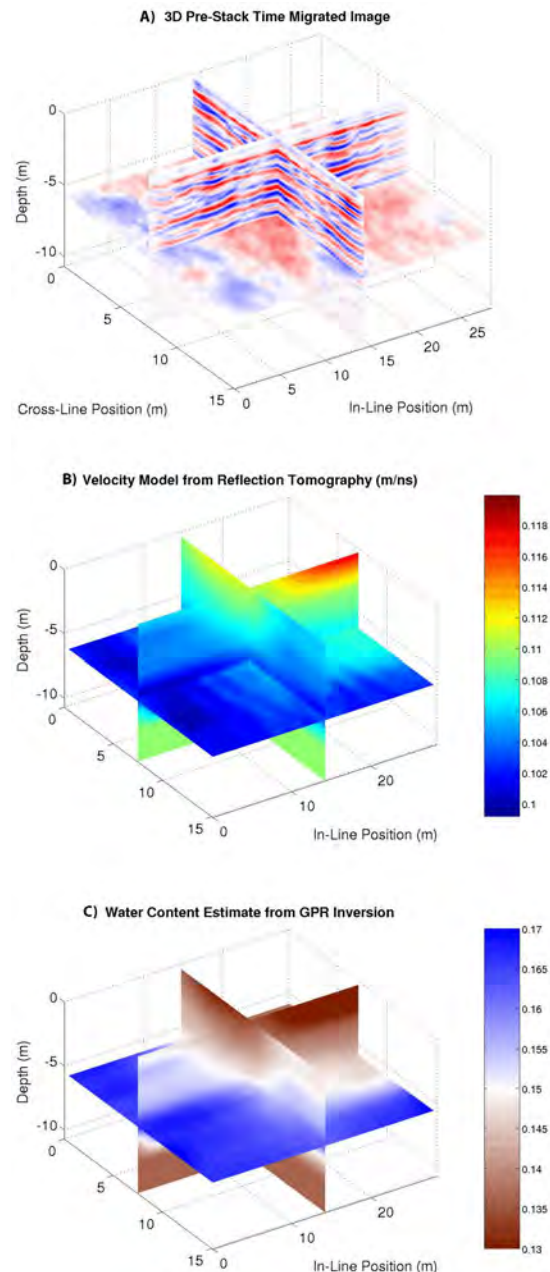
Figure 3: A) 3D pre-stack time migrated image at the Hanford site. The image shows a detailed stratigraphy of the upper 6m with a channel along the left side of the volume. B) The velocity model from tomography shows significant 3D variability. C) An increase in water content, computed using the Topp equation, is evident within a stratigraphic layer from 4 - 6m. Water content increases toward the left and front of the volume.